



Effect of summer snow cover on the active layer thermal regime and thickness on CALM-S JGM site, James Ross Island, eastern Antarctic Peninsula

Filip Hrbáček^{a,*}, Zbyněk Engel^{b,1}, Michaela Kňázková^a, Jana Smolíková^{a,b}

^a Department of Geography, Faculty of Science, Masaryk University, Brno, Czech Republic

^b Department of Physical Geography and Geoecology, Faculty of Science, Charles University, Prague, Czech Republic

ARTICLE INFO

Keywords:

Antarctica
Soils
Periglacial environment
Ground penetrating radar
Ground temperature

ABSTRACT

This study aims to assess the role of ephemeral snow cover on ground thermal regime and active layer thickness in two ground temperature measurement profiles on the Circumpolar Active Layer Monitoring Network – South (CALM-S) JGM site on James Ross Island, eastern Antarctic Peninsula during the high austral summer 2018. The snowstorm of 13–14 January created a snowpack of recorded depth of up to 38 cm. The snowpack remained on the study site for 12 days in total and covered 46% of its area six days after the snowfall. It directly affected ground thermal regime as indicates temperature record at snow-covered profile AWS-JGM which subsurface section was nearly 5 °C colder compared to the snow-free AWS-CALM profile. The thermal insulation effect of snow cover is also reflected in the mean monthly (January) and summer (DJF) ground temperatures on AWS-JGM that decreased by ca 1.1 and 0.7 °C, respectively. Summer thawing degree days at a depth of 5 cm decreased by ca 10% and active layer was ca 5–10 cm thinner when compared to previous snow-free summer seasons. Surveying by ground penetrating radar revealed a general active layer thinning of up to 20% in those parts of the CALM-S which were covered by snow of >20 cm depth for at least six days.

1. Introduction

Seasonal occurrence of snow cover, its thickness and spatial distribution significantly affect ground thermal regime as well as active layer refreezing in regions underlain by permafrost. It is estimated that a snow accumulation about 40 cm deep has the maximum insulating effect (e.g., Zhang, 2005). Generally, thinner snow accumulation tends to have a cooling effect on the ground while a thicker and long-lasting snow cover can increase the ground temperature. The insulating effect of snow cover in permafrost conditions is the most prominent in winter due to maximum snow thickness, high surface albedo and the porosity of snow, and a large temperature difference between the atmosphere and the ground surface (Harris et al., 2009; Callaghan et al., 2011). Under these conditions, the solar energy absorbed by the snow surface is reduced, thermal conduction within the snowpack is low, and the transfer of heat between the air and the soil surface is limited. The net influence of snow over the cold period amounts to an increase of mean ground temperatures and maximum thaw depths, but these effects vary greatly in space

and time (Zhang, 2005). At the end of winter the insulating effect of snow decreases, and meltwater becomes the primary influence.

During the summer period, the effect of snow on ground temperature and thaw depth is considered to be relatively small under permafrost conditions (Goodrich, 1982). The ground remains frozen underneath long-lasting snow patches but warms rapidly in snow-free areas (Harris and Corte, 1992). The infiltration of meltwater increases the thermal conductivity of the ground, enhancing heat transfer from the ground surface to the permafrost table (Campbell et al., 1998). When ephemeral snow cover builds up during the summer, snow protects the ground from warm air and the active layer may eventually refreeze from the permafrost table upwards. However, this cooling effect is limited and its impact on the ground is controlled primarily by the duration of the snow cover, snow properties and a temperature difference between the air and the ground surface. The insulating capacity of snow increases in late summer when the thaw plane tends to rise rapidly (Goodrich, 1982). The impact of summer snow cover on ground temperatures and active layer thickness was studied rarely in the high mountains (Hoelzle et al., 2003;

* Corresponding author.

E-mail address: hrbacekfilip@gmail.com (F. Hrbáček).

¹ Both authors contributed equally to this paper.

Luetschg et al., 2008; Magnin et al., 2017; Mena et al., 2021), arctic environment (Christiansen, 2004; Hinkel and Hurd, 2006; Park et al., 2015) and Maritime Antarctic (Guglielmin and Cannone, 2012; Guglielmin et al., 2014b; de Pablo et al., 2017; Ramos et al., 2017, 2020). Most of these studies deal with the cooling effect of a delayed snow cover melt due to its albedo and the latent heat flux. Changes in the ground thermal regime induced by summer snowfall events were reported only from the Alps (Hanson and Hoelzle, 2004; Draebing et al., 2017; Magnin et al., 2017), Tianshan Mountains (Zhao et al., 2018) and arid Andes in Chile (Mena et al., 2021).

The snow cover effect on ground thermal regime or active layer thawing has been widely studied in the Arctic regions during the past decades (e.g., Zhang, 2005; Callaghan et al., 2011; Johansson et al., 2013; Park et al., 2015). However, the knowledge on snow-ground interactions in Antarctica is limited mostly to sites within the Antarctic Peninsula region (AP) with only a few studies from different parts of the continent. Generally, snowpack controls the ground thermal regime and active layer thickness in Antarctica in different ways depending on its seasonal duration and prevailing depth. Only a negligible effect of winter snowpack on ground thermal regime was observed in dry and cold conditions of the north-eastern AP where snow cover in winter is irregular and usually thinner than 30 cm (Hrbáček et al., 2016). A ground temperature increase was observed in cases when snow persists for the majority of the winter with a thickness between 30 and 70 cm. Such conditions are characteristic for the study sites on the South Shetlands in the north-western AP (Oliva et al., 2017a; de Pablo et al., 2017; Ramos et al., 2017) and they were also observed in topographically similar sites on James Ross Island (Kňažková et al., 2020). Importantly, ground warming during the thaw season can lead to permafrost degradation especially in areas on the border conditions between continuous and discontinuous permafrost of the north-western AP (Hrbáček et al., 2020).

At the same time, however, persistent snowpack can lead to active layer thinning and its effect can eventually promote permafrost aggradation. The main reason is a shortening of the thawing season (Ramos et al., 2017). Consequently, the heat deficit reduces active layer thawing propagation. Such conditions were observed on the South Shetlands after 2010 (de Pablo et al., 2017; Ramos et al., 2017) and they were related to a recent climate cooling (Turner et al., 2016; Oliva et al., 2017b) and an associated increase in snow precipitation within the AP region (Carrasco and Cordero, 2020). Similar effect of long-lasting snow

cover was reported from the Victoria Land where the presence of snow prevented the active layer from thawing in the summer completely (Guglielmin et al., 2014a). General cooling of the active layer and permafrost was further observed in areas where snowpack exceeded 1 m, as reported by Guglielmin et al. (2014b) from Adelaide Island. According to Ramos et al. (2020), permanent accumulation of >4.5 m can even lead to a complete insulation of the ground from atmosphere, causing permafrost aggradation and forming a specific subnival thermal regime of the ground.

This study brings a new perspective on the effect of snow on ground thermal regime and active layer thickness. We assess the role of a relatively thick ephemeral snowpack that occurred in the high summer 2018 on the area of Circumpolar Active Layer Monitoring site (CALM-S) JGM on James Ross Island. The objectives of this study are to (i) describe the spatial variability of snow cover thickness in the study area in January 2018, (ii) assess the differences in ground thermal regime and active layer thickness between the snow-covered and snow-free sites, and (iii) determine the effect of ephemeral snowpack on active layer thaw depth.

2. Study area

James Ross Island is located in the north-eastern sector of the AP (Fig. 1). The northern part of James Ross Island, Ulu Peninsula, constitutes the largest ice-free area in the entire AP. The mean annual air temperature (MAAT) in the lowland parts of JRI (<50 m asl) was $-7.0\text{ }^{\circ}\text{C}$ in the period 2006–2015 with a positive trend of annual temperatures but a cooling trend in the summer (DJF) months (Hrbáček and Uxa, 2020). The annual precipitation is estimated to about 300–700 mm w.e.y^{-1} (van Wessem et al., 2016; Palermé et al., 2017). Snow cover is distributed irregularly as indicated by perennial snowfields on lee-slopes and snow patches around topographic obstacles. Snow thickness in the flat lowland areas is usually less than 20 cm, but can rarely exceed 40 cm (Hrbáček et al., 2016; Kňažková et al., 2020). The ice-free area is underlain by continuous permafrost with a modelled temperature between $-4\text{ }^{\circ}\text{C}$ and $-8\text{ }^{\circ}\text{C}$ (Obu et al., 2020). The active layer thickness strongly depends on lithology and varies between 50 and 120 cm (Hrbáček et al., 2019).

The study site is located on the CALM-S JGM which is the part of a continental database under code A27 (CALM-S database, 2021). The area of 80 m by 70 m was established in February 2014 following recommendations for CALM-S sites proposed by Guglielmin (2006). The

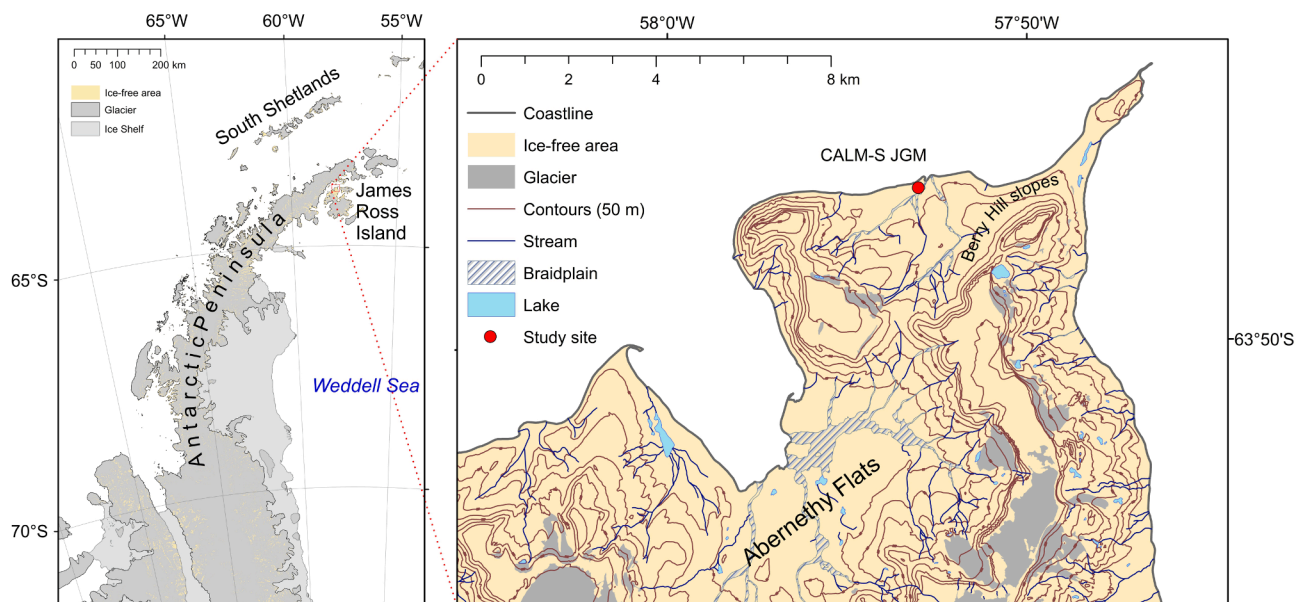


Fig. 1. Regional setting (left) and the location of CALM-S JGM site (right).

area comprises diverse geological units, with a Holocene marine terrace covering ca 80% of the northern part of the site and Cretaceous Whisky Bay Fm. forming the remaining 20% of the site (Fig. 2). The geological conditions lead to a variability of general ground physical characteristics and consequently drive the variability of active layer thaw depth which is about 20 cm thicker in the southern part underlain by the Cretaceous sediments (Hrbáček et al., 2017).

3. Material and methods

3.1. Temperature monitoring and data processing

There are two automatic weather stations (AWS) installed within the CALM-S JGM grid. The fully equipped site AWS-JGM is located in the part formed by the marine terrace. It provides data on air temperature at 2 m above ground measured by Pt100/8 sensor (accuracy ± 0.15 °C) placed in a radiation shield, and ground temperature measured by Pt100/8 thermometers (accuracy ± 0.15 °C) placed directly in the ground. The second automatic weather station (AWS-CALM) is installed in the Cretaceous sediments about 60 m to the west from AWS-JGM and provides data on ground temperature only. The measurement is conducted by the same thermistors and placed at the same depths as on AWS-JGM. Missing data in the AWS-CALM record in the period 18 December 2016 to 20 January 2017 were replaced using a multiple regression according to air and ground temperature data from AWS-JGM. With regards to the size of the CALM-S JGM area, the air temperatures from AWS-JGM site are considered to be representative also for AWS-CALM (Hrbáček et al., 2017).

Climate data were analysed for the austral summer periods 2016/17 and 2017/18. Particularly, the following parameters were calculated:

- Daily and seasonal mean air and ground temperatures at depths of 5, 50 and 75 cm;
- Thawing degree days of air and (TDD_A) ground at a depth of 5 cm (TDD_5) calculated as a sum of positive daily temperatures;
- Isothermal days at a depth of 5 cm set as an event with the maximum and minimum daily temperatures within the interval 0.5 °C to -0.5 °C (Guglielmin, 2006).

Further, we evaluated 30 min variability of air, and ground temperatures at depths of 5, 50 and 75 cm and 2 h variability of snow depth in the period from 10 January to 25 January 2018. The daily variability of active layer thickness (ALT) was defined as a maximum daily depth of 0 °C isotherm for the entire period of thawing season and the maximum seasonal ALT is calculated accordingly.

3.2. ALT measurements

Mechanical probing and ground penetrating radar (GPR) soundings were used to determine seasonal changes of active layer thickness. Thaw depths were measured on 31 January and 12 February during the summer period 2016/17 and on 20 January, 12 and 24 February in the 2017/18 summer period. The gridded sampling design with evenly distributed nodes at 10 m spacing was used for the probing, which was carried out at each of the grid nodes with a 1 cm diameter steel rod of 120 cm length. GPR data were collected along nine parallel profiles with north–south orientation, four profiles (Fig. 2) were selected for a detailed analysis. GPR sounding was carried out using a shielded 500 MHz antenna and RAMAC CU-II control unit (MALÅ GeoScience, 2005). A wheel encoder was used to trig the measurements and control the distance along the profiles. The time window was set to 54.6 ns and scan spacing to 0.049 m. GPR data were processed using the REFLEXW software version 8.5 (Sandmeier, 2017). The depth axis of raw GPR profiles was converted from the time axis using the wave velocity determined from thaw depths probed at grid nodes and from the position of relevant reflector in GPR scans. The velocity obtained for each sampling date ranged between 0.071 and 0.094 m ns⁻¹ increasing towards the late summer season with decreasing soil moisture (Fig. 3a). This velocity range and the electromagnetic pulse width yield a maximum vertical (depth) resolution length of 4–5 cm, assuming a resolution of one quarter of the GPR signal wavelength (Knapp, 1990). The position of the permafrost table is actually determined less precisely due to changes in water content within active layer associated with various sediment types, grain size, porosity and compaction (e.g. Jol and Bristow, 2003). To cover uncertainties in the location of a target, the vertical resolution is usually approximated by half of the signal wavelength (Luo et al., 2019), which corresponds to the range of 7–9 cm in case of the 500 MHz antennae and the above-mentioned velocity

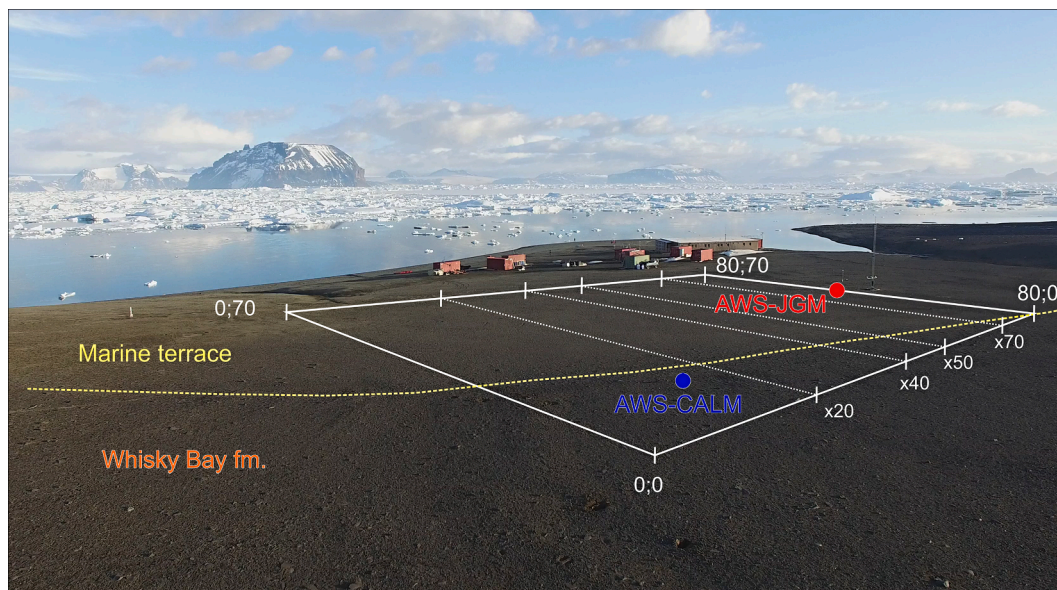


Fig. 2. Study site from the south-west. The white polygon with local coordinates (x;y) in the corners delimits the area of CALM-S JGM, white dotted lines indicate selected ground penetrating radar profiles shown in Fig. 7, and the yellow dotted line represents the boundary between the geological formations of Holocene marine terrace and Cretaceous Whisky Bay Fm. Colour points represent positions of ground temperature monitoring profiles. (For interpretation of the references to colour in this figure legend, the reader is referred to the web version of this article.)

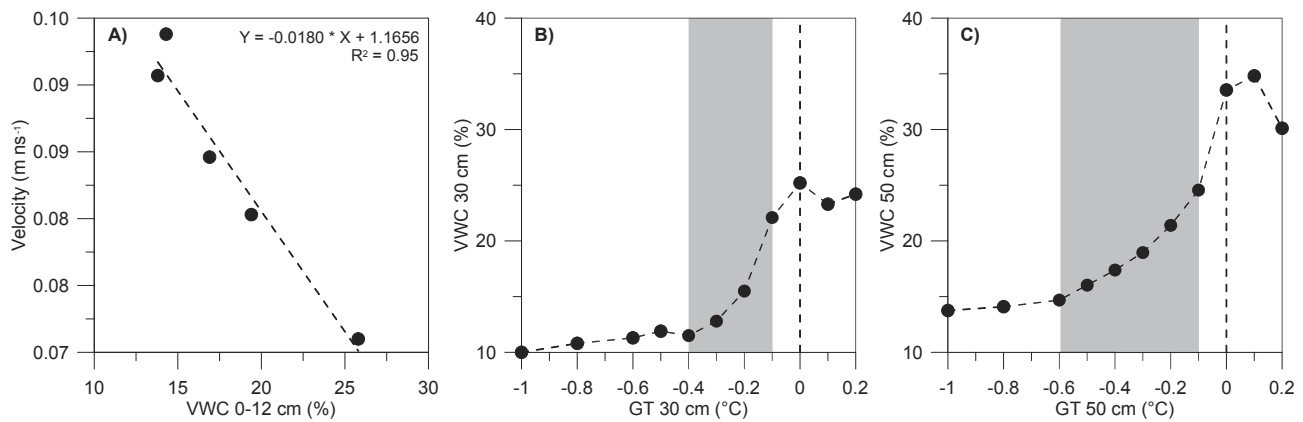


Fig. 3. Linear correlation is observed between mean surficial volumetric water content (VWC) on CALM-S JGM and GPR wave velocities in active layer (A). Relationship between mean volumetric water content and associated mean ground temperature (GT) at 30 cm (B) and 50 cm (C) depth indicates the temperature interval of soil water phase change (shaded rectangle).

range. The volumetric soil moisture was set as a mean value of 72 measurements recorded at each grid point of CALM-S JGM within 12 cm thick subsurface layer of the ground using the HydroSense II measuring device paired with the CS658 soil–water sensor (Campbell Scientific, Inc.). Volumetric water content measured by CS650 sensor (Campbell Scientific, Inc.) in the depths of 30 and 50 cm was used together with ground temperature records on AWS-CALM to construct the soil freezing curves. The active layer phase change occurred between -0.1 °C and -0.6 °C (Fig. 3b, c) reflecting the variability in salt content in the ground, which may decrease the freezing point temperature nearly by 2 °C (Harris et al., 2018).

3.3. Snow cover observations

A long-term year-round monitoring of snow depths is provided at 2-hour interval using the Judd (accuracy ± 1 cm) ultrasonic sensor installed at the AWS-JGM since 2011 (Hrbáček et al., 2016). The sensor is located within 5-meter distance from ground temperature measurement profile. Raw readings from the sensor were corrected against actual air temperatures following the specification of the manufacturer (Judd Communication). Snow depth data are available for the summer season 2017/18 due to sensor failure prior to the summer 2016/17.

The extent of snow cover in the 2017/2018 summer was identified using an unmanned aerial vehicle (UAV) imagery. DJI Phantom 3 Professional was used for the survey at a flight height of 30 m allowing the ground sample distance of approximately 1.0 cm. Pictures from the UAV were processed and orthorectified in Metashape (Agisoft) and used for the delimitation of snow patches in ArcMap 10.4 (ESRI). The spatial distribution of snow depth was assessed based on the GPR scanning and mechanical probing. The scanning with a shielded 800 MHz antenna was carried out along nine parallel GPR profiles designed for ALT measurements and probing was done at a rectangular array of the CALM-S grid nodes with a steel rod covering both the ice-covered and bare parts of the test site. The signal acquisition time of GPR scanning was set to 38.1 ns and scan spacing to 0.019 m. The probed snow depths were used to adjust the position of snow/ground interface in obtained GPR scans allowing for a precise conversion of time axis to depth, and interpolation of snow depth using the Radial Basis Function in Surfer 15 (Golden Software).

4. Results

4.1. Air temperatures during the period 2016–2018

Data from the AWS-JGM site provide a general understanding of climate conditions at the study site over the period 2016–2018. MAAT

ranged from -6.7 °C to -3.9 °C with a mean temperature of -5.5 °C for the 3-year period. The value of -3.9 °C obtained for the year 2016 represents the highest annual air temperature recorded at the study site since the beginning of measurements in 2004. The warmest year was followed by significantly colder year 2017 with the MAAT of -6.7 °C, which is, however, only 0.1 °C colder compared to the mean air temperature for the period 2004–2018. The year 2018 with the MAAT of -5.8 °C belongs to warmer years in the AWS-JGM temperature record.

Mean summer air temperatures over the investigated period coincide within the measurement uncertainty of temperature sensors, varying between 0.1 °C in 2016/17 and 0.0 °C in 2017/18. Similarly, mean monthly air temperatures for the warmest month (January) ranged from 0.2 °C (2016/17) to -0.1 °C (2017/18). Mean daily air temperatures mostly varied between 5.0 °C and -2.0 °C (Fig. 4) and the warmest period occurred at the turn of January and February in both summer seasons. Summer TDD_A reached 83 °Cdays in 2016/17 and 67 °Cdays in 2017/18 (Table 1).

The most prominent cooling over the summer period 2017/18 was connected with the snowstorm event that occurred on 13 to 14 January 2018. The air temperature decreased from above-zero values to -5.4 °C immediately after the snowstorm but remained rather positive with a mean of 1.0 °C from 16 to 25 January. Fig. 4b shows air temperature variation during this event and its effect on ground temperatures at snow covered/snow free sites. While air temperature controlled ground temperature fluctuations at bare ground, it did not affect subsurface temperatures below the snow cover.

4.2. Ground thermal regime in the summer seasons 2016/17 and 2017/18

Mean seasonal ground temperatures on AWS-JGM ranged from 4.3 °C (2016/17) and 3.4 °C (2017/18) at a depth of 5 cm to -1.2 °C (2016/17) and -1.4 °C (2017/18) at a depth of 75 cm. Mean daily temperatures at a depth of 5 cm were mostly positive with the maximum values exceeding 10.0 °C in 2016/17 and 8.0 °C in 2017/18 (Fig. 4a). Isothermal days at a depth of 5 cm occurred only twice in 2016/17, whereas 9 such days were observed in 2017/18 (Table 1). The summer TDD₅ were 398 °C days (2016/17) and 311 °C days (2017/18). The detailed view on the ground thermal regime in January 2018 (Fig. 4a) indicates that the temperature at the depth of 5 cm remained between -0.2 °C and -0.3 °C under the snow cover >10 cm deep. Over the same period, the ground temperature at the depth of 50 cm decreased from positive (0.1 to 0.4 °C) to negative values of -0.3 °C. The snowpack melted earlier at the site of ground temperature measurement than below the ultrasonic snow depth sensor (Fig. 5). Therefore, the ground temperature regime shows positive values with typical daily regime

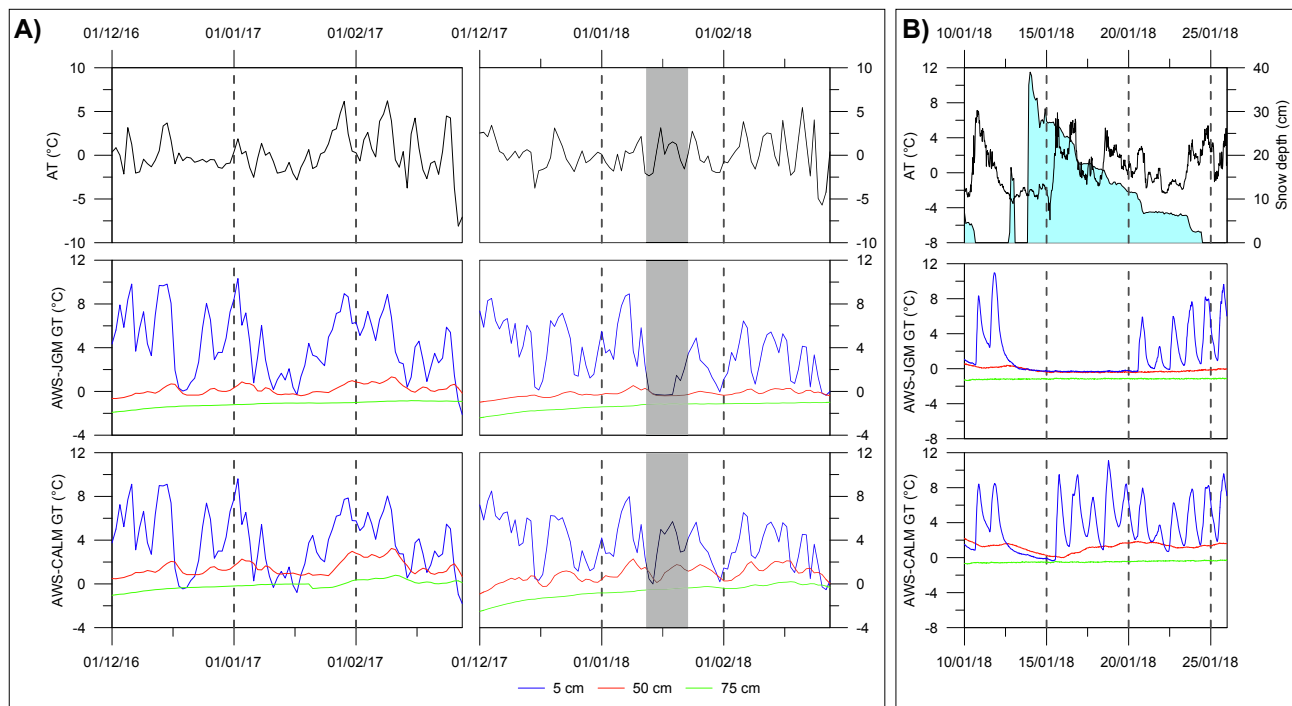


Fig. 4. Variability of air temperature (AT) and ground temperatures (GT) at depths of 5, 50 and 75 cm on AWS-JGM and AWS-CALM. Temperatures are presented as daily means of summer seasons 2016/17 and 2017/18 (A) and 30-min records in the period 10 January to 25 January 2018 (B). Grey rectangle in plot A) indicates the period with compact snow cover detected on AWS-JGM.

Table 1

Selected thermal characteristics of air temperature (AT) and ground temperature at a depth of 5 cm (GT₅) on AWS-JGM and AWS-CALM in the summer periods 2016/17 and 2017/18.

Season	Period	AT	TDD _A	AWS-JGM			AWS-CALM		
				GT ₅	TDD ₅	ITD*	GT ₅	TDD ₅	ITD*
2016/17	DJF	0.1	83	4.3	398	2	3.9	354	0
	January	0.2	26	4.0	117	0	3.5	101	0
2017/18	DJF	0.0	67	3.4	311	9	3.8	340	1
	January	-0.1	17	2.8	82	9	3.7	112	1

* ITD = isothermal days.

since 21 January, three days before the snow completely melted.

Different pattern of mean seasonal ground temperatures was observed on AWS-CALM. While the temperature at a depth of 5 cm differed only slightly between 3.9 °C (2016/17) and 3.8 °C (2017/18), the differences in the depths of 50 and 75 cm were greater. Observed means were 1.5 °C (2016/17) and 0.9 °C (2017/18) at a depth of 50 cm and -0.1 °C (2016/17) and -0.7 °C (2017/18) at 75 cm. Mean daily temperatures at a depth of 5 cm only rarely dropped below 0 °C (Fig. 4). Their seasonal maximums exceeded 8.5 °C (2016/17) and 6.5 °C (2017/18). Only one isothermal day appeared in the season 2017/18. The summer TDD₅ were 354 °Cdays (2016/17) and 340 °Cdays (2017/18). The ground temperature at the depth of 5 cm dropped to -0.4 °C after the cooling and snowstorm event in January 2018. However, the temperature ranged from 1.2 °C and 11.1 °C for the rest of the period with snow presence on AWS-JGM. The temperature at the depth of 50 cm decreased from 2.2 °C (10 January) to 0.0 °C (16 January), but it increased rapidly up to 2.0 °C (21 January) as the snow cover melted.

4.3. Snow cover at CALM-S JGM site in January 2018

Snowstorm occurred between 13 January 22:00 UTC and 14 January 4:00 UTC. A relatively short period of 6 hr was sufficient to create snow cover that reached a maximum depth of 38 cm at AWS-JGM site. The

most rapid thinning of the snowpack was observed on the 16 January when the snow depth decreased by 8 cm as a result of relatively high air temperatures that reached 6.0 °C in maximum (Fig. 4b). Snow persisted until 24 January when the last shallow snowpack (3 cm) melted (Fig. 4b).

The distribution and thickness of snow were surveyed six days after the snowstorm, when snow cover extent was reduced to 46% of the CALM-S JGM area. The ground plan of the snow patch was complex and snow depth variable (Fig. 5) due to the redistribution by strong wind during the snowstorm and irregular melting after the storm. Snow drift produced irregular pattern of elongated zastrugi features and inter-leaving troughs with the SW-NE orientation. Owing to the drift, snow depth ranged from 20 to 30 cm on the ridges to less than 5 cm in troughs. While the maximum snow depths determined at probed profiles was 25 cm, the modelled mean snow depth was 10 cm. Within the snow patch, wind-blown ground appeared at seven places that increased rapidly in extent due to the enhanced snowmelt on the margins of bare ground.

4.4. Evolution of ALT during summer seasons 2016/17 and 2017/18

The active layer thawing in 2016/17 begun in early October, while it started around mid-November in 2017/18. The most rapid thawing propagation in the early thawing season at the turn of November and

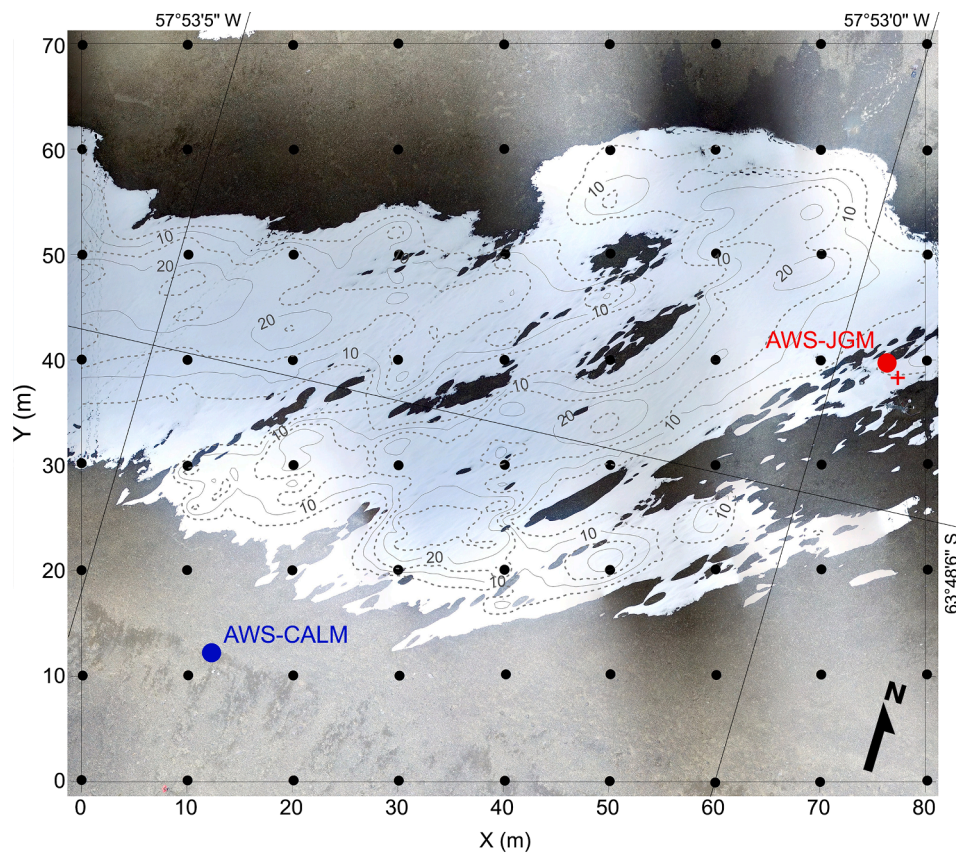


Fig. 5. Distribution of snow with 5 cm isohyets of snow depth on CALM-S JGM on 20th January 2018. Black points mark 10 m grid nodes, colour points represent the position of ground temperature measurement profiles AWS-JGM (red) and AWS-CALM (blue), red cross represents the position of snow depth sensor on AWS-JGM. The image was derived from a UAV flight. (For interpretation of the references to colour in this figure legend, the reader is referred to the web version of this article.)

December was connected with a rapid increase in total TDD₅ during this period (Fig. 6). Thaw depths were around 50 cm (AWS-JGM) and 65 cm (AWS-CALM) in mid-December when the thawing propagation started to slow down (Fig. 6). The most pronounced interruption of thawing

progress was observed on AWS-JGM in January 2018 when the active layer refroze completely after a snowstorm. The maximum thicknesses on AWS-JGM reached 66 cm (10 February 2017) and 59 cm (8 January 2018). Observed maximums on AWS-CALM were 90 cm (11 February

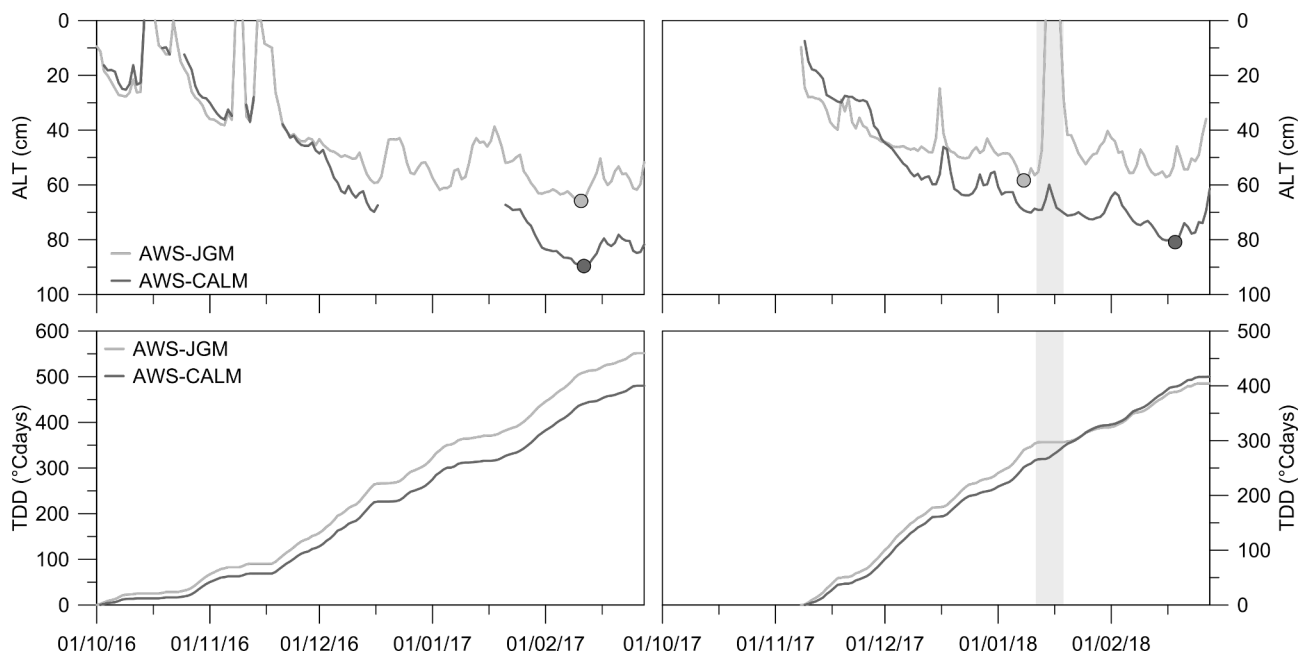


Fig. 6. Seasonal evolution of active layer thickness (ALT) and thawing degree days (TDD₅) on AWS-JGM and AWS-CALM in the seasons 2016/17 and 2017/18. Dots indicate maximum active layer thickness on both AWS sites. Grey rectangle indicates the period with compact snow cover detected on AWS-JGM.

2017) and 81 cm (18 February 2018). Total TDD₅ in thawing seasons reached 552 °C days (2016/17) and 404 °C days (2017/18) on AWS-JGM. The TDD₅ on AWS-CALM were 512 °C days (2016/17) and 416 °C days (2017/18).

The difference in ALT between the two subsequent summer seasons is clearly visible in Fig. 7 that also reveals relatively even thaw plane during the summer 2016/17 and its irregular course in January 2018. The largest interannual difference in thaw depths coincides with those sections of the scanned profiles that were covered with thick continuous snowpack during the January 2018 measurement in profiles X20 and X40 (Fig. 7). Within these sections, the thaw plane is located 20 to 30 cm higher compared to the snow-free parts of the profiles. The thaw plane along the predominantly snow-free profile 70 in January 2018 is more or less parallel to the permafrost table observed in 2017 (Fig. 7). This is also the case of February measurements in all measured profiles. The observed discrepancy between zero thaw depth values (Fig. 6) and detected active layer thickness (Fig. 7) is explained by the fact, that the actual active layer freezing temperature is lower than 0 °C (Fig. 3b, c). Therefore, we were able to detect unfrozen active layer even under negative ground temperature conditions (Fig. 4b).

Spatial distribution of thaw depth for the CALM-S JGM site during the late summer 2016/17 and 2017/18 is illustrated in Fig. 8. Thaw depths were more spatially uniform in February 2017 although two geologically distinct parts of the study area are clearly visible. The bimodal distribution with prevailing lower ALT (less than 80 cm) and

thaw depths as high as 115 cm along the southern margin of the study area have already been observed over the years 2014–16. This large contrast in thaw depth has been tentatively attributed to different grain size distribution and moisture content in two sedimentary units within the study area (Hrbáček et al., 2017). The strongly bimodal pattern can be seen in the 2018 grid that shows even more pronounced difference in thaw depths between the two parts. The region of decreased ALT coincides with maximum snow depths in January 2018 that is also consistent with the difference between mean thaw depths over the period 2014–17 and 2018 grid (Fig. 8D).

5. Interpretation and discussion

5.1. Climate conditions in the study area in the context of previous years

Air temperatures in the study area during the summer periods 2016/17 and 2017/18 were below long-term (2006–2015) summer average of 0.4 °C reported for the AWS-JGM and nearby Abernethy Flats sites (Hrbáček and Uxa, 2020). Although the lowest mean air temperature on CALM-S site was recorded in the summer 2014/15 (Hrbáček et al., 2017), the lowest TDDA was observed in 2017/18 (Table 2) indicating a decrease in a total number of days with prevailing positive temperatures. The mean summer ground temperatures at a depth of 5 cm were the lowest in the season 2017/18. By contrast to the previous summer seasons when both summer and January ground temperature was 0.1 to

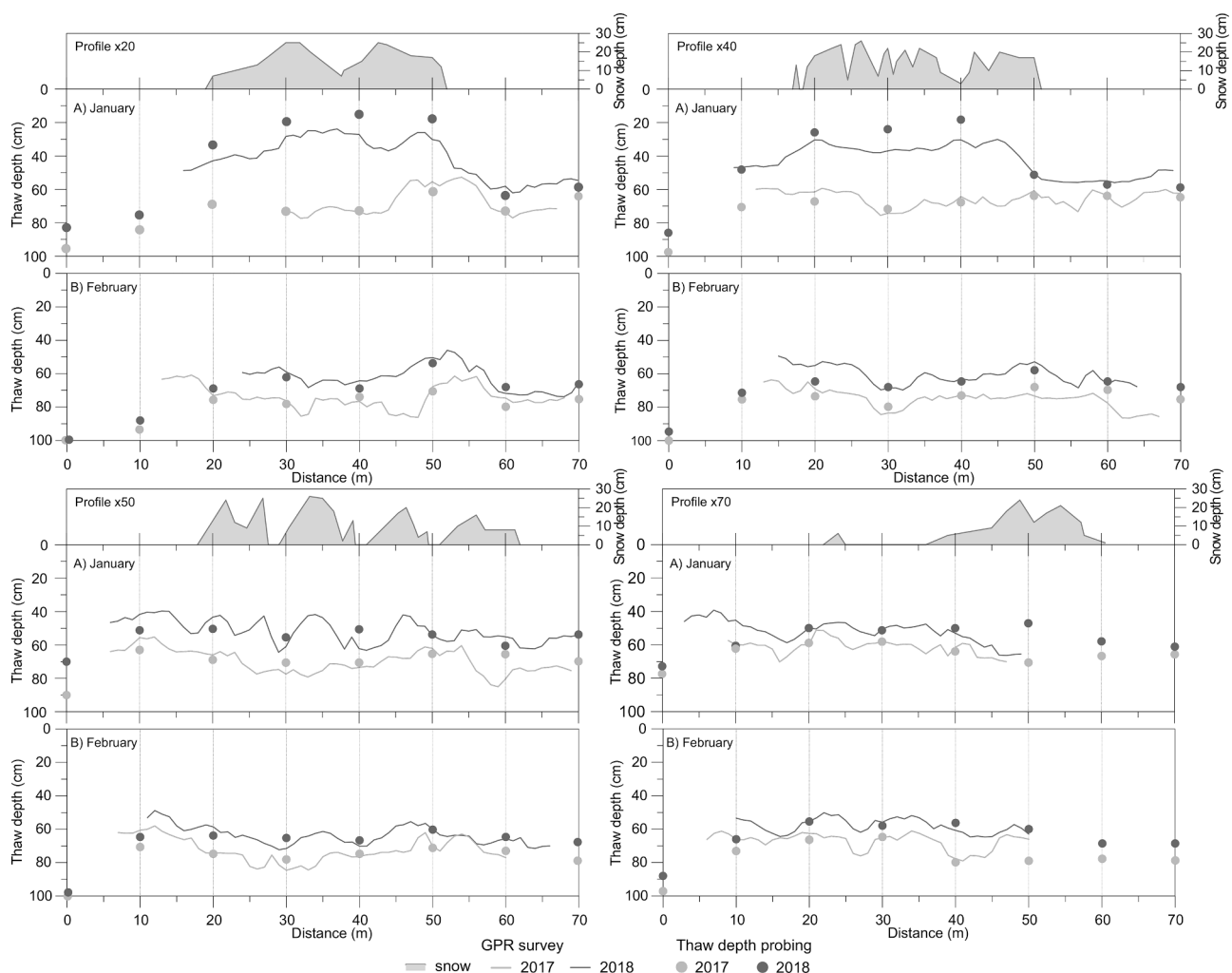


Fig. 7. Snow cover depth (grey polygons) in January 2018 and thaw depths in January and February 2017 and 2018 determined from GPR and probing measurements at CALM-S JGM site.

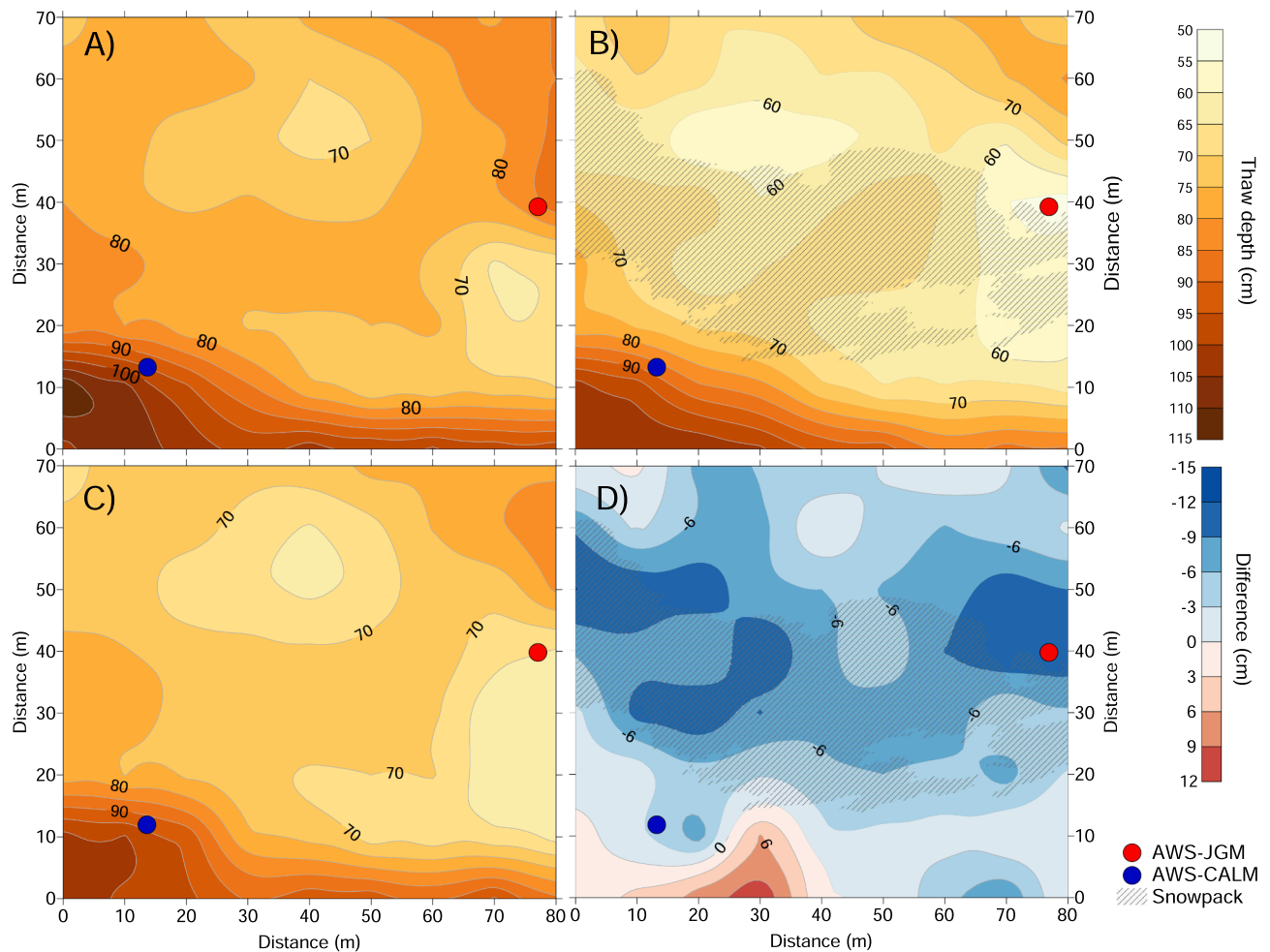


Fig. 8. Spatial variability of thaw depth on CALM-S JGM in A) February 2017, B) February 2018, C) mean thaw depth in the period 2014–2017 and D) difference between February 2018 and the 2014–2017 mean.

Table 2

Variability of mean summer (DJF) of air temperature (AT) and ground temperature (GT) at the depth of 5 cm, thawing degree days of ground (TDD₅) and active layer thickness (ALT) on AWS-JGM and AWS-CALM in the period 2014/15 to 2017/18.

Season	AT DJF (°C)	GT DJF AWS- CALM (°C)	GT DJF AWS- CALM (°C)	TDD ₅ AWS- JGM (°Cdays)	TDD ₅ AWS- CALM (°Cdays)	ALT AWS- JGM (cm)	ALT AWS- CALM (cm)
2014/ 15*	-0.5	4.7	4.4	456	418	63	86
2015/ 16*	0.4	4.7	4.6	506	478	65	87
2016/ 17	0.1	4.3	3.9	552	502	67	90
2017/ 18	0	3.4	3.8	404	416	59	82

* Data according to Hrbáček et al. (2017).

0.5 °C higher on AWS-JGM than AWS-CALM, we observed opposite pattern during the summer 2017/18. The ground temperature was 0.4 °C (DJF) to 0.9 °C (January) higher on AWS-CALM than AWS-JGM (Fig. 9). We associated this unusual pattern with the presence of snow cover during January 2018 which caused the differences of the mean daily ground temperatures up to 6.0 °C and the 30-min temperatures even up to 11.4 °C (Fig. 4a, b).

Regardless of relatively cold summer ground surface temperatures, the thickest active layer and the highest TDD₅ on both AWS-JGM and AWS-CALM were observed in 2016/17 (Table 2). This was primarily caused by unusually warm spring months (September to November) in the north-eastern part of the AP (Turner et al., 2020). Such conditions favoured early melting of the active layer in the beginning of October which started weeks earlier than usually (Hrbáček et al., 2017; Hrbáček and Uxa, 2020). Sandy soil texture together with lower moisture also supports warmer surficial conditions on AWS-JGM as documented by TDD₅ higher by 28–50 °Cdays than on AWS-CALM. However, TDD₅ were 12 °C days lower in 2017/18 on AWS-JGM than on AWS-CALM (Fig. 9).

5.2. Snow cover effect on ground thermal regime

Variations in summer air temperature and the length of the thaw season control ALT but snow cover may reduce it significantly (e.g., Guglielmin, 2004; Zhang, 2005; Guglielmin et al., 2012). While a cooling effect of thick long-lasting snow patches has been reported from different regions including AP (Guglielmin et al., 2014b; Ramos et al., 2017, 2020), the influence of thin snow cover that rapidly builds and melts during the warm period remains poorly known. The ground thaw depths recorded in January 2018 at the CALM-S JGM site demonstrate a decrease in active layer thickness underneath ephemeral snow cover with limited depth that protected the ground surface only for six days prior to ALT measurements. The initial maximum snow depth of 38 cm falls within the range of 30–70 cm that is considered sufficient to isolate the ground from temperature variations (e.g., de Pablo et al., 2017;

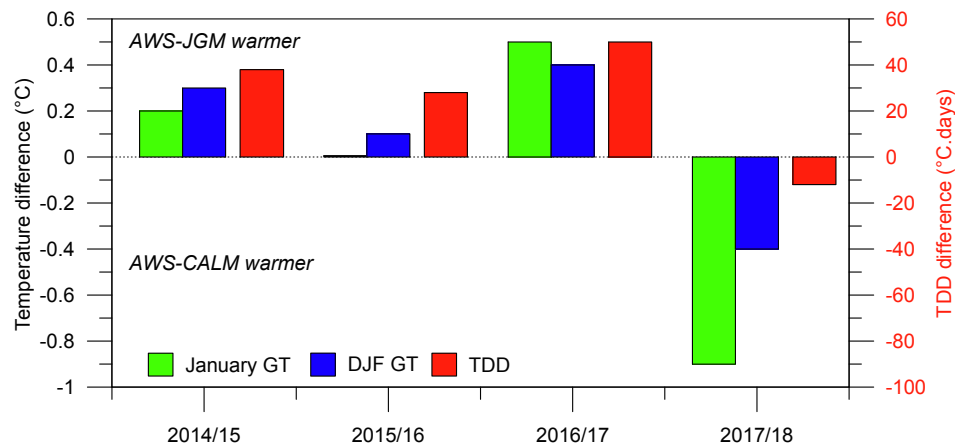


Fig. 9. Difference in ground temperature (GT) and thawing degree days (TDD) between AWS-JGM and AWS-CALM in the period 2014/15 to 2017/18. Data from period 2014/15 and 2015/16 adopted from Hrbáček et al. (2017).

Kňažková et al., 2020). However, the maximum snow depth of 25 cm observed on the CALM-S JGM at the time of ALT measurements indicates much lower snow depth over most of the study area. Considering that ALT thinning was observed far beyond the margin of the snowpack, a mean snow depth of 10 cm has sufficient influence on the ground thermal regime. This value is significantly lower than the effective snow depth of 20 cm considered with respect to the insulation effect of snow in AP region (de Pablo et al., 2016; Oliva et al., 2017a). This suggests that main impact of ephemeral summer snow cover on ground temperature results from the strong reflection of solar radiation due to high albedo of the snow surface rather than from the insulating effect of a thin snowpack.

The largest impact of ephemeral snow cover on thaw depths in the study area can be seen underneath thick continuous snowpack in profiles X20 and X40 (Fig. 7), where active layer thinning reaches 20 to 30 cm. By contrast, a slight overall decrease (lower than 10 cm) in ALT was observed along profile X50 across irregularly thick snowpack with frequent holes and at predominantly snow-free profile X70 (Fig. 7). The difference in thaw depths between snow-covered and bare surface decreases rapidly after the snowmelt. The snow cover disappeared from the study area on 24 January and measurements from 12 February reveal the unimodal distribution of ALT. The rapid restoration of a more or less uniform thaw plane results from the combination of relatively high air temperatures and an enhanced conduction of heat from the ground surface due to meltwater percolation (*sensu* de Pablo et al., 2014; Farzamián et al., 2020). The influence of ephemeral snow cover on thaw depths is apparent in the timing of the maximum ALT on snow-covered and bare sites. Whereas the maximum ALT on snow-affected AWS-JGM site was observed before the snowstorm event on 9 January, the ALT maximum on a snow-free site occurred on 18 February. The later culmination of the thaw depth at the snow-free site coincides well with the timing of the maximum ALT in previous summer seasons which is typically around mid-February (Hrbáček et al., 2017).

The ground temperatures recorded at the CALM-S JGM indicate that ephemeral snow cover may also affect thermal regime of the active layer. As Fig. 4 shows, the presence of snow cover with an initial depth of 38 cm eliminates diurnal temperature fluctuations down to a depth of 50 cm and results in a substantial decrease in the mean daily ground temperatures. The mean monthly ground surface temperature in January is reduced by nearly one degree below the snow cover (with the depth decreasing from 38 to 12 cm over six days) compared to the bare surface (Tables 1 and 2). Although the net cooling effect of ephemeral snow over the summer season is limited, the number of isothermal days increases and TDD₅ are reduced by ca 10% compared to snow-free summer seasons (Tables 1 and 2). This is in line with the reported insulating effect of snow patches that persist over the warm season in

permafrost conditions (de Pablo et al., 2017). Guglielmin et al. (2014b) and Oliva et al. (2017a) reported a cooling of the ground surface and a reduced magnitude of ground temperature fluctuations on Adelaide Island, western AP; and Livingston Island, north-western AP, respectively. De Pablo et al. (2017) observed an increase in the minimum ground surface temperatures below quasi-permanent snow patches on Livingston Island, north-western AP. The observed changes in recorded ground temperatures confirm that the presence of snow cover may be more important for the active layer refreezing and thaw plane position than summer temperatures (Zhang, 2005; de Pablo et al., 2017; Ramos et al., 2017). This also implies that the seasonal active-layer measurement should not be done immediately after summer snowfall events.

5.3. Assessment of the results in a wider regional context

The previous studies on JRI considered the winter snowpack as too thin and temporally unstable to create a sufficient insulation layer on the ground (Hrbáček et al., 2016). This is mostly because of dynamic weather conditions during winter and prevailing strong southern winds which remove the snow from flat surfaces resulting in its irregular distribution within the terrain (Kavan et al., 2020). In specific conditions of long-lasting snow accumulations, a snowpack >30 cm deep causes isothermal regime of ground temperature during the winter months (Kňažková et al., 2020).

Most of the studies dealing with relationships between snow and the ground thermal regime in Antarctica are located in the South Shetlands in the north-western AP. The oceanic climate makes this part of AP one of the wettest regions in Antarctica with precipitation rates of >1000 mm yr⁻¹ (Carrasco and Cordero, 2020). This results in high annual net snow accumulation and snow cover depth, with mean values of about 0.5 m (de Pablo et al., 2017). Such snowpack can cause a significant warming of the ground compared to windswept areas (Oliva et al., 2017a). As the northern AP is located in border conditions between continuous and discontinuous permafrost (Bockheim et al., 2013; Obu et al., 2020), regular and thick snowpack in the winter months can lead to permafrost degradation (Hrbáček et al., 2020). On the other hand, mean annual air temperature has decreased at a statistically significant rate since the beginning of the 20th century, with a most rapid cooling during the summer season (Turner et al., 2016, Oliva et al., 2017b). This was reflected in an increase in the number of snowfall events on the north-western side of the AP since the mid-2010s during the summer period (Carrasco and Cordero, 2020). Despite the fact that the trends in the annual total of precipitation from extreme precipitation events over 1979–2016 are small (Turner et al., 2019), positive trends in the precipitation total and summer snowfall events may result in a more frequent accumulation of ephemeral snow cover with a temporary

cooling effect.

This study brings new insight into the functioning of the snow cover in relation to active layer thickness. So far, the active layer thinning was attributed mostly to long-lasting snow accumulation which prevented active layer thawing during the early warm season. Therefore, its thinning was directly related to the shortening of the thawing season (Ramos et al., 2017; de Pablo et al., 2017). Consequently, the long-term active layer thinning rate was more likely connected with an increased duration of the snow cover in the northwestern AP, rather than with the climate variability during summer months (Ramos et al., 2017, 2020). In other Antarctic regions, like Victoria Land, snowpack can persist for an entire summer and completely prevent active layer thawing (Guglielmin et al., 2014a). However, the ephemeral snowpack's role in summer has not been described yet from neither Antarctic nor Arctic regions. The influence of summer snowfalls and related snowpack on the thermal regime and thickness of the active layer has been reported from alpine areas (Magnin et al., 2017; Zhao et al., 2018; Mena et al., 2021), but snow and ground conditions in the mountains differ strongly from those in high latitudes (Hoelzle and Gruber, 2008). Usually, the period of high summer is characterized by a low snowfall intensity and predominantly bare ground surface in ice-free areas across Antarctica. Therefore, snowfall events leading to an accumulation of >30 cm deep snow cover are scarce in this region and the snow control on ground thermal regime is primarily related to its high albedo.

6. Conclusions

This study brings a new perspective on the effect of snow cover on active layer thermal regime and thickness in the Antarctic Peninsula region. The recent research deals mostly with the role of winter or permanent snow cover, whereas the role of ephemeral snow occurring during the high summer was not documented at all in Antarctica. This study shows that even short-term presence of a relatively thick snow cover during the high summer can significantly affect active layer thermal regime and thawing propagation. Considering the observations from 2017/18 within the context of the snow-free seasons with similar air temperature conditions, the ephemeral snow cover considerably affected the ground thermal regime and active layer thickness. The magnitude of the snow insulation effect was controlled by the snow depth and duration of snowpack. The observed snowpack with an initial snow depth of 38 cm lasted for 12 days during the high summer season. Below the ephemeral snow cover, the diurnal temperature fluctuations were limited down to a depth of 50 cm, thaw depths decreased by nearly 20%, the maximum active layer thickness was observed almost six weeks prior to the maximum on a snow-free site, and the mean monthly ground temperature was reduced by nearly one degree compared to the snow-free surface. The number of isothermal days increased and TDD₅ were reduced by ca 10% in the presence of snow cover.

Declaration of Competing Interest

The authors declare that they have no known competing financial interests or personal relationships that could have appeared to influence the work reported in this paper.

Acknowledgement

The research was supported by the Ministry of Education, Youth and Sports of the Czech Republic projects LM2015078 and CZ.02.1.01/0.0/0.0/16_013/0001708; by the Masaryk University project MUNI/A/1517/2020; and by the Czech Science Foundation project GC20-20240S. The authors acknowledge the crew of JGM station, particularly Jakub Ondruch for providing UAV imagery and Kamil Laska for the support on the meteorological measurements setting and maintenance.

References

- Bockheim, J., Vieira, G., Ramos, M., López-Martínez, J., Serrano, E., Guglielmin, M., Wilhelm, K., Nieuwendam, A., 2013. Climate warming and permafrost dynamics in the Antarctic Peninsula region. *Glob. Planet. Change* 100, 215–223. <https://doi.org/10.1016/j.gloplacha.2012.10.018>.
- Callaghan, T.V., Johansson, M., Brown, R.D., Groisman, P.Y., Labba, N., Radionov, V., Bradley, R.S., Blangy, S., Bulygina, O.N., Christensen, T.R., Colman, J.E., Essery, R.L.H., Forbes, B.C., Forchhammer, M.C., Golubev, V.N., Honrath, R.E., Juday, G.P., Meshcherskaya, A.V., Phoenix, G.K., Pomeroy, J., Rautio, A., Robinson, D.A., Schmidt, N.M., Serreze, M.C., Shevchenko, V.P., Shiklomanov, A.I., Shmakin, A.B., Skold, P., Sturm, M., Woo, M.K., Wood, E.F., 2011. Multiple effects of changes in arctic snow cover. *Ambio* 40, 32–45. <https://doi.org/10.1007/s13280-011-0213-x>.
- Campbell, I.B., Claridge, G.G.C., Campbell, D.I., Balks, M.R., 1998. The Soil Environment of the McMurdo Dry Valleys, Antarctica. In: Prisco, J.C., (Ed.), *Ecosystem Dynamics in a Polar Desert: the McMurdo Dry Valleys, Antarctica*. Am. Geophys. Union, Washington. <https://doi.org/10.1029/AR072p0297>.
- Carrasco, J.F., Cordero, R.R., 2020. Analyzing precipitation changes in the northern tip of the Antarctic Peninsula during the 1970–2019 period. *Atmosphere* 11 (12), 1270. <https://doi.org/10.3390/atmos11121270>.
- Christiansen, H.H., 2004. Meteorological control on interannual spatial and temporal variations in snow cover and ground thawing in two northeast Greenlandic Circumpolar-Active-Layer-Monitoring (CALM) sites. *Permafrost Periglac.* 15, 155–169. <https://doi.org/10.1002/ppp.489>.
- de Pablo, M.A., Ramos, M., Molina, A., 2014. Thermal characterization of the active layer at the Linnopolare Lake CALM-S site on Byers Peninsula (Livingston Island), Antarctica. *Solid Earth* 5, 721–739. <https://doi.org/10.5194/se-5-721-2014>.
- de Pablo, M.A., Ramos, M., Molina, A., Vieira, G., Hidalgo, M.A., Prieto, M., Jiménez, J.J., Fernández, S., Recondo, C., Calleja, J.F., Peón, J.J., Mora, C., 2016. Frozen ground and snow cover monitoring in the South Shetland Islands, Antarctica: instrumentation, effects on ground thermal behaviour and future research. *Cuad. Investig. Geográfica* 42, 475–495.
- de Pablo, M.A., Ramos, M., Molina, A., 2017. Snow cover evolution, on 2009–2014, at the Linnopolare lake CALM-S site on Byers peninsula, Livingston island, Antarctica. *Catena* 149, 538–547. <https://doi.org/10.1016/j.catena.2016.06.002>.
- Draebing, D., Haberkorn, A., Krautblatter, M., Kenner, R., Phillips, M., 2017. Thermal and mechanical responses resulting from spatial and temporal snow cover variability in permafrost rock slopes, Steintaeli. *Swiss Alps. Permafrost Periglac.* 28 (1), 140–157. <https://doi.org/10.1002/ppp.v28.110.1002/ppp.1921>.
- Farzaman, M., Vieira, G., Monteiro Santos, F.A., Yaghoobi Tabar, B., Hauck, C., Catarina Paz, M., Bernardo, I., Ramos, M., Angel De Pablo, M., 2020. Detailed detection of active layer freeze-thaw dynamics using quasi-continuous electrical resistivity tomography (Deception Island, Antarctica). *Cryosphere* 14, 1105–1120. <https://doi.org/10.5194/tc-14-1105-2020>.
- Goodrich, L.E., 1982. The influence of snow cover on the ground thermal regime. *Can. Geotech. J.* 19 (4), 421–432. <https://doi.org/10.1139/82-047>.
- Guglielmin, M., 2004. Observations on permafrost ground thermal regimes from Antarctica and the Italian Alps, and their relevance to global climate change. *Glob. Planet. Change* 40 (1–2), 159–167. [https://doi.org/10.1016/S0921-8181\(03\)00106-1](https://doi.org/10.1016/S0921-8181(03)00106-1).
- Guglielmin, M., 2006. Ground surface temperature (GST), active layer and permafrost monitoring in continental Antarctica. *Permafrost Periglac.* 17 (2), 133–143. [https://doi.org/10.1002/\(ISSN\)1099-153010.1002/ppp.v17.210.1002/ppp.553](https://doi.org/10.1002/(ISSN)1099-153010.1002/ppp.v17.210.1002/ppp.553).
- Guglielmin, M., Cannone, N., 2012. A permafrost warming in a cooling Antarctica? *Clim. Change* 111 (2), 177–195. <https://doi.org/10.1007/s10584-011-0137-2>.
- Guglielmin, M., Worland, M.R., Cannone, N., 2012. Spatial and temporal variability of ground surface temperature and active layer thickness at the margin of maritime Antarctica, Signy Island. *Geomorphology* 155, 20–33. <https://doi.org/10.1016/j.geomorph.2011.12.016>.
- Guglielmin, M., Dalle Fratte, M., Cannone, N., 2014a. Permafrost warming and vegetation changes in continental Antarctica. *Environ. Res. Lett.* 9 (4), 045001. <https://doi.org/10.1088/1748-9326/9/4/045001>.
- Guglielmin, M., Worland, M.R., Baio, F., Convey, P., 2014b. Permafrost and snow monitoring at Rothera Point (Adelaide Island, Maritime Antarctica): implications for rock weathering in cryotic conditions. *Geomorphology* 225, 47–56. <https://doi.org/10.1016/j.geomorph.2014.03.051>.
- Hanson, S., Hoelzle, M., 2004. The thermal regime of the active layer at the Murtèl rock glacier based on data from 2002. *Permafrost Periglac.* 15 (3), 273–282. [https://doi.org/10.1002/\(ISSN\)1099-153010.1002/ppp.v15.310.1002/ppp.499](https://doi.org/10.1002/(ISSN)1099-153010.1002/ppp.v15.310.1002/ppp.499).
- Harris, C., Arenson, L.U., Christiansen, H.H., Etzelmüller, B., Frauenfelder, R., Gruber, S., Haeblerli, W., Hauck, C., Hölzle, M., Humlum, O., Isaksen, K., Käab, A., Kern-Lüschtig, M.A., Lehning, M., Matsuoka, N., Murton, J.B., Nötzli, J., Phillips, M., Ross, N., Seppälä, M., Springman, S.M., Vonder Mühll, D., 2009. Permafrost and climate in Europe: monitoring and modelling thermal, geomorphological and geotechnical responses. *Earth-Science Rev.* 92 (3), 117–171. <https://doi.org/10.1016/j.earscirev.2008.12.002>.
- Harris, S.A., Corte, A.E., 1992. Interactions and relations between mountain permafrost, glaciers, snow and water. *Permafrost Periglac.* 3 (2), 103–110. [https://doi.org/10.1002/\(ISSN\)1099-153010.1002/ppp.v3.210.1002/ppp.3430030207](https://doi.org/10.1002/(ISSN)1099-153010.1002/ppp.v3.210.1002/ppp.3430030207).
- Harris, S.A., Brouckov, A., Guodong, C., 2018. *Geocryology: Characteristics and Use of Frozen Ground and Permafrost Landforms*. CRC Press, London, p. 765.
- Hinkel, K.M., Hurd, J.K., 2006. Permafrost destabilization and thermokarst following snow fence installation, Barrow, Alaska, USA. *Arct. Antarct. Alp. Res.* 38 (4), 530–539. [https://doi.org/10.1657/1523-0430\(2006\)38\[530:PDATFS\]2.0.CO;2](https://doi.org/10.1657/1523-0430(2006)38[530:PDATFS]2.0.CO;2).
- Hoelzle, M., Gruber, S., 2008. Borehole and ground surface temperatures and their relationship to meteorological conditions in the Swiss Alps. In: Kane, D.L., Hinkel, K.

- M. (Eds.), 9th International Conference on Permafrost, 29 June – 03 July 2008, Fairbanks, Alaska. Institute of Northern Engineering, Fairbanks, pp. 723–728. <https://doi.org/10.5167/uzh-2825>.
- Hoelzle, M., Haeberli, W., Stocker-Mittaz, C., 2003. Miniature ground temperature data logger measurements 2000–2002 in the Murtèl-Corvatsch area. In: Phillips, M., Springman, S., Arenson, L. (Eds.), Proceedings of the 8th International Conference on Permafrost. Swets & Zeitlinger, Lisse, pp. 419–424.
- Hrbáček, F., Láška, K., Engel, Z., 2016. Effect of snow cover on the active-layer thermal regime – a case study from James Ross Island, Antarctic Peninsula. *Permafrost Periglac.* 27 (3), 307–315. <https://doi.org/10.1002/ppp.v27.310.1002/ppp.1871>.
- Hrbáček, F., Kňazková, M., Nývlt, D., Láška, K., Mueller, C.W., Ondruch, J., 2017. Active layer monitoring at CALM-S site near J.G. Mendel station, James Ross Island, eastern Antarctic Peninsula. *Sci. Total Environ.* 601–602, 987–997. <https://doi.org/10.1016/j.scitotenv.2017.05.266>.
- Hrbáček, F., Nývlt, D., Láška, K., Kňazková, M., Kampová, B., Engel, Z., Oliva, M., Mueller, C.W., 2019. Permafrost and active layer research on James Ross Island: An overview. *Czech Polar Reports* 9 (1), 20–36. <https://doi.org/10.5817/CPR2019-1-3>.
- Hrbáček, F., Oliva, M., Fernández, J.-R., Kňazková, M., de Pablo, M.A., 2020. Modelling ground thermal regime in bordering (dis)continuous permafrost environments. *Environ. Res.* 181, 108901. <https://doi.org/10.1016/j.envres.2019.108901>.
- Hrbáček, F., Uxa, T., 2020. The evolution of a near-surface ground thermal regime and modelled active-layer thickness on James Ross Island, Eastern Antarctic Peninsula, in 2006–2016. *Permafrost Periglac.* 31, 141–155. <https://doi.org/10.1002/ppp.2018>.
- Johansson, M., Callaghan, T.V., Bosiò, J., Åkerman, H.J., Jackowicz-Korczynski, M., Christensen, T.R., 2013. Rapid responses of permafrost and vegetation to experimentally increased snow cover in sub-arctic Sweden. *Environ. Res. Lett.* 8 (3), 035025. <https://doi.org/10.1088/1748-9326/8/3/035025>.
- Jol, H.M., Bristow, C.S., 2003. GPR in sediments: advice on data collection, basic processing and interpretation, a good practice guide. In: Bristow, C.S., Jol, H.M. (Eds.), *Ground Penetrating Radar in Sediments*. Geol. Soc. Spec. Publ., London, pp. 9–27. <https://doi.org/10.1144/GSL.SP.2001.211.01.02>.
- Judd Communications, 2011. Judd Communications Depth Sensor. Available at: <http://static1.1.sqspcdn.com/static/f/1146254/15414722/1322862508567/ds2m anual.pdf>. (accessed 31 January 2020).
- Kavan, J., Nývlt, D., Láška, K., Engel, Z., Kňazková, M., 2020. High-latitude dust deposition in snow on the glaciers of James Ross Island, Antarctica. *Earth Surf. Proc. Land.* 45 (7), 1569–1578. <https://doi.org/10.1002/esp.v45.710.1002/esp.4831>.
- Knapp, R.W., 1990. Vertical resolution of thick beds, thin beds and thin-bed cyclothem. *Geophysics* 55 (9), 1183–1190. <https://doi.org/10.1190/1.1442934>.
- Kňazková, M., Hrbáček, F., Kavan, J., Nývlt, D., 2020. Effect of hyaloclastite breccia boulders on meso-scale periglacial-aeolian landsystem in semi-arid antarctic environment, James Ross Island, Antarctic Peninsula. *Geogr. Res. Lett.* 46, 7–31.
- Luetschg, M., Lehning, M., Haeberli, W., 2008. A sensitivity study of factors influencing warm/thin permafrost in the Swiss Alps. *J. Glaciol.* 54 (187), 696–704. <https://doi.org/10.3189/002214308786570881>.
- Luo, T.X.H., Lai, W.W.L., Chang, R.K.W., Goodman, D., 2019. GPR imaging criteria. *J. Appl. Geophys.* 165, 37–48. <https://doi.org/10.1016/j.jappgeo.2019.04.008>.
- Magnin, F., Westermann, S., Pogliotti, P., Ravanel, L., Deline, P., Malet, E., 2017. Snow control on active layer thickness in steep alpine rock walls (Aiguille du Midi, 3842 m a.s.l., Mont Blanc massif). *Catena* 149 (2), 648–662. <https://doi.org/10.1016/j.catena.2016.06.006>.
- MALÁ GeoScience, 2005. Ramac GPR. Hardware manual. Malá: MALÁ GeoScience.
- Mena, G., Yoshikawa, K., Schorghofer, N., Pastén, C., Ochoa, F.A., Yoshii, Y., Doi, M., Miyata, T., Takahashi, H., Casassa, G., Sone, T., 2021. Freeze–thaw cycles and snow impact at arid permafrost region in Chajnantor Volcano, Atacama, northern Chile. *Arct. Antarct. Alp. Res.* 53 (1), 60–66. <https://doi.org/10.1080/15230430.2021.1878739>.
- Obu, J., Westermann, S., Vieira, G., Abramov, A., Balks, M.R., Bartsch, A., Hrbáček, F., Kääh, A., Ramos, M., 2020. Pan-Antarctic map of near-surface permafrost temperatures at 1 km² scale. *Cryosphere* 14, 497–519. <https://doi.org/10.5194/tc-14-497-2020>.
- Oliva, M., Hrbáček, F., Ruiz-Fernández, J., de Pablo, M.Á., Vieira, G., Ramos, M., Antoniadis, D., 2017a. Active layer dynamics in three topographically distinct lake catchments in Byers Peninsula (Livingston Island, Antarctica). *Catena* 149, 548–559. <https://doi.org/10.1016/j.catena.2016.07.011>.
- Oliva, M., Navarro, F., Hrbáček, F., Hernández, A., Nývlt, D., Perreira, P., Ruiz-Fernández, J., Trigo, R., 2017b. Recent regional climate cooling on the Antarctic Peninsula and associated impacts on the cryosphere. *Sci. Total Environ.* 580, 210–223. <https://doi.org/10.1016/j.scitotenv.2016.12.030>.
- Palermo, C., Genthon, C., Claud, C., Kay, J.E., Wood, N.B., L'Ecuyer, T., 2017. Evaluation of current and projected Antarctic precipitation in CMIP5 models. *Clim. Dyn.* 48 (1–2), 225–239. <https://doi.org/10.1007/s00382-016-3071-1>.
- Park, Hotaek, Fedorov, Alexander N., Zheleznyak, Mikhail N., Konstantinov, Pavel Y., Walsh, John E., 2015. Effect of snow cover on pan-Arctic permafrost thermal regimes. *Clim. Dyn.* 44 (9–10), 2873–2895. <https://doi.org/10.1007/s00382-014-2356-5>.
- Ramos, M., Vieira, G., de Pablo, M.A., Molina, A., Abramov, A., Goyanes, G., 2017. Recent shallowing of the thaw depth at Crater Lake, Deception Island, Antarctica (2006–2014). *Catena* 149 (2), 519–528. <https://doi.org/10.1016/j.catena.2016.07.019>.
- Ramos, M., Vieira, G., de Pablo, M.A., Molina, A., Jimenez, J.J., 2020. Transition from a Subaerial to a Subnival Permafrost Temperature Regime Following Increased Snow Cover (Livingston Island, Maritime Antarctic). *Atmosphere* 11, 1332. <https://doi.org/10.3390/atmos11121332>.
- Sandmeier, K.J., 2017. Reflexw Processing Program for Seismic, Acoustic and Electromagnetic Reflection, Refraction and Transmission Data, Version 8.5. Sandmeier Scientific Software, Karlsruhe.
- Turner, J., Lu, H., White, I., King, J.C., Phillips, T., Hosking, J.S., Bracegirdle, T.J., Marshall, G.J., Mulvaney, R., Deb, P., 2016. Absence of 21st century warming on Antarctic Peninsula consistent with natural variability. *Nature* 535 (7612), 411–415. <https://doi.org/10.1038/nature18645>.
- Turner, J., Phillips, T., Thamban, M., Rahaman, W., Marshall, G.J., Wille, J.D., Favier, V., Winton, V. H.L., Thomas, E., Wang, Z., Broeke, M., Hosking, J.S., Lachlan-Cope, T., 2019. The dominant role of extreme precipitation events in Antarctic snowfall variability. *Geophys. Res. Lett.* 46 (6), 3502–3511. <https://doi.org/10.1029/2018GL081517>.
- Turner, J., Marshall, G.J., Clem, K., Colwell, S., Phillips, T., Lu, H., 2020. Antarctic temperature variability and change from station data. *Int. J. Climatol.* 40 (6), 2986–3007. <https://doi.org/10.1002/joc.v40.610.1002/joc.6378>.
- van Wessem, J.M., Ligtenberg, S.R.M., Reijmer, C.H., van de Berg, W.J., van den Broeke, M.R., Barrand, N.E., Thomas, E.R., Turner, J., Wuite, J., Scambos, T.A., van Meijgaard, E., 2016. The modelled surface mass balance of the Antarctic Peninsula at 5.5 km horizontal resolution. *Cryosphere* 10, 271–285. <https://doi.org/10.5194/tc-10-271-2016>.
- Zhang, T., 2005. Influence of the seasonal snow cover on the ground thermal regime: An overview. *Rev. Geophys.* 43, RG4002. <https://doi.org/10.1029/2004RG000157>.
- Zhao, J.Y., Chen, J., Wu, Q.B., Hou, X., 2018. Snow cover influences the thermal regime of active layer in Urumqi River Source, Tianshan Mountains. *China. J. Mt. Sci.* 15 (12), 2622–2636. <https://doi.org/10.1007/s11629-018-4856-y>.